Author Manuscript

Author Manuscript

Author Manuscript

Author Manuscript

HHS Public Access

Author manuscript

Cancer Res. Author manuscript; available in PMC 2018 December 01.

Published in final edited form as:

Cancer Res. 2017 December 01; 77(23): 6641–6650. doi:10.1158/0008-5472.CAN-16-3452.

MYC Inhibition depletes cancer stem-like cells in triple-negative breast cancer

Aim in Yang[1], **Shenghui Qin**[1], **Bradley A. Schulte**[1], **Stephen P. Ethier**[1], **Kenneth D. Tew**[2], and **Gavin Y. Wang**[1]

[1]Department of Pathology and Laboratory Medicine, Medical University of South Carolina, Charleston, SC 29425, USA

[2]Department of Cell and Molecular Pharmacology & Experimental Therapeutics, Medical University of South Carolina, Charleston, SC 29425, USA

Abstract

There is mounting evidence that cancer stem-like cells (CSCs) are selectively enriched in residual tumors after anticancer therapies which may account for tumor recurrence and metastasis by regenerating new tumors. Thus, there is a critical need to develop new therapeutic agents that can effectively eliminate drug-resistant CSCs and improve the efficacy of cancer therapy. Here we report that Triptolide (C1572), a small molecule natural product selectively depletes CSCs in a dose-dependent fashion in human triple-negative breast cancer (TNBC) cell lines. Nanomolar concentrations of C1572 markedly reduced c-MYC (MYC) protein levels via a proteasome-dependent mechanism. Silencing MYC expression phenocopied the CSC depletion effects of C1572 and induced senescence in TNBC cells. Limited dilution assays revealed that ex vivo treatment of TNBC cells with C1572 reduced CSC levels by 28-fold. In mouse xenograft models of human TNBC, administration of C1572 suppressed tumor growth and depleted CSCs in a manner correlated with diminished MYC expression in residual tumor tissues. Together, these new findings provide a preclinical proof of concept defining C1572 as a promising therapeutic agent to eradicate CSCs for drug-resistant TNBC treatment.

Keywords

c-MYC; Cancer stem cells; Triple-negative breast cancer; Triptolide

Introduction

Breast cancer is the most frequently diagnosed form of cancer and the second leading cause of cancer-related death among women both in the United States and worldwide (1). Gene expression profiling has identified several distinct molecular subtypes of breast cancers including luminal A and B, HER 2 positive, basal-like and normal-like (2, 3). Approximately 70% of the triple negative breast tumors are identified as the basal-like

Correspondence to: Gavin Y. Wang, MD, PhD, Department of Pathology and Laboratory Medicine, Medical University of South Carolina, 171 Ashley Avenue, MSC908, Charleston, SC 29425, Tel: 1-843-792-9983; Fax: 1-843-792-0368, wangy@musc.edu.

Conflict of Interest: The authors declare no conflict of interest

Author Manuscript Author Manuscript Author Manuscript Author Manuscript

subtype (4). Despite recent advances in breast cancer treatment, targeted therapeutics for triple-negative breast cancer (TNBC) do not exist because this subtype lacks druggable targets such as hormone receptors and amplified HER 2 expression (5). Anthracyclines and Taxanes based chemotherapy is a standard of care for TNBC treatment. However, sooner or later TNBC patients will experience drug resistance, tumor relapse and/or metastasis after a transient response to initial rounds of therapies (5–8). Thus, there is an urgent need to develop innovative and more effective therapeutic approaches that achieve a more durable response to TNBC treatment.

Cancer stem-like cells (CSCs), also known as tumor-initiating cells (TICs), have the unique ability to self-renew, differentiate and generate the diverse cells that comprise the tumor. Previous studies have demonstrated that CSCs are highly tumorigenic, as few as 100 CSCs are able to form tumors when xenotransplanted into immunocompromised mice, whereas tens of thousands of non-tumorigenic cancer cells do not (9, 10). Thus, CSCs are thought to be the underlying cause of tumor recurrence and metastasis by giving rise to new tumors (11, 12). Furthermore, it appears that CSCs are resistant to current anticancer therapies, as demonstrated by the fact that they are selectively enriched in residual tumors after chemotherapy and/or radiation therapy (7, 8, 13–15). These new observations strongly suggest that the inability of current cancer therapies to eliminate CSCs in heterogeneous tumors may account for relapse and treatment failure. Thus, targeting of CSCs may represent a novel therapeutic strategy for improving the efficacy of cancer treatment. However, there is currently no FDA-approved therapeutics that can effectively eradicate drug-resistant CSCs in TNBC treatment.

Dysregulation of the *MYC* oncogene has been implicated in the pathogenesis of a variety of human cancers, including TNBC (16–19). Interestingly, MYC overexpression is associated with poor outcomes in breast cancer (19). Evidence also exists that elevated MYC expression is particularly common in the triple-negative subtype of breast cancers (18, 20, 21). MYC is a transcriptional target of Wnt/β-catenin and activation of the Wnt/β-catenin signaling pathway has been linked to CSC self-renewal in basal-like breast cancer (22, 23). Notably, MYC has been shown to be a key factor required for stem cell reprogramming (24). Furthermore, recent studies have suggested that MYC is required for β-catenin-mediated mammary stem cell amplification and tumorigenesis (25). However, it is not known if targeting MYC is a valid therapeutic strategy to eradicate drug-resistant CSCs for breast cancer therapy.

C1572, also known as Triptolide, was originally isolated from the medicinal vine Tripterygium wilfordii Hook F which has been used in traditional Chinese medicine for centuries (26), particularly for the treatment of a variety of autoimmune diseases and as an immuno-suppressant in patients with organ and tissue transplantations (27–29). Minnelide is a water-soluble prodrug of C1572 that has been shown to exhibit promising tumor suppression effects in pancreatic cancer, although the mechanism(s) of action are elusive (30). Interestingly, C1572 also can protect mice against cisplatin-induced acute kidney injury and alleviate autosomal dominant polycystic kidney disease via stimulating calcium (Ca^{2+}) channel polycystin-2 mediated Ca^{2+} release (26, 31).

Author Manuscript Author Manuscript Author Manuscript Author Manuscript

In the present study, through unbiased drug screen we have identified C1572 as a promising lead compound that selectively depletes drug-resistant CSCs via targeting MYC in human TNBC cells. Strikingly, our results reveal that C1572 is 100-fold more potent than the commercially available small-molecule inhibitor of MYC, JQ1 (32), in inhibiting MYC in TNBC cells. Furthermore, our studies have demonstrated for the first time that C1572-mediated tumor growth suppression and CSC depletion correlate well with a marked inhibition of MYC expression in residual TNBC xenograft tumor tissues. Collectively, these results suggest that pharmacologic inhibition of MYC by C1572 may represent a novel and effective therapeutic approach for eliminating drug-resistant CSCs in TNBC.

Methods and Materials

Ethics statement

All preclinical animal studies were performed in compliance with the regulations and ethical guidelines for experimental animal studies of the Institutional Animal Care and Use Committee (IACUC) at the Medical University of South Carolina (Charleston, SC).

Materials

SUM149 and SUM159 human TNBC cell lines were developed by Dr. Stephen Ethier. We received these cell lines directly from Dr. Ethier lab and the cells were maintained as previously described (33, 34). The MDA-MB-231 human breast cancer cell line was purchased from American Type Culture Collection. The cells were cultured in DMEM medium containing 10% FBS, 2 mM L-glutamine and 100 microgram/mL of penicillin-streptomycin (Invitrogen). Cell authentication was performed by short tandem repeat assays. Dulbecco's modified Eagle's medium (DMEM), DMEM/F12 medium, recombinant human basic fibroblast growth factor (bFGF) and B27 supplement were obtained from Invitrogen (Carlsbad, CA).

Mammosphere formation assay

Mammosphere formation assays were performed to determine the sphere-forming activity of CSCs as previously described (35–37). Briefly, single-cell suspensions prepared from human TNBC cell lines or TNBC xenograft tumors were cultured at 2000 to 5000 cells/mL per well in 24-well ultra-low attachment plates (Corning) using serum-free DMEM/F-12 medium supplemented with 20 ng/mL basic FGF, 20 ng/mL EGF, 4 μg/mL insulin, 4 μg/mL heparin, 0.5 μg/mL hydrocortisone, 0.4% BSA and B27 (Invitrogen). Culture medium was replaced every other day with 50% fresh medium. Tumor spheres were counted and photographed after 7 days of culture.

siRNA transfection

To knockdown MYC expression, human TNBC cells were transfected with MYC-specific siRNAs (Qiagen, Valencia, CA) using Lipofectamine RNAi MAX (Invitrogen) according to the manufacturer's protocol. AllStars negative control siRNAs (Qiagen, Valencia, CA) were used as controls. At 48 h after transfection, MYC expression levels in transfected cells were assessed by Western blot analyses.

Author Manuscript Author Manuscript Author Manuscript Author Manuscript

Senescence-associated β-galactosidase (SA-β-gal) staining

In situ staining of SA-β-gal was performed using a senescence β-galactosidase staining kit (Cell Signaling) to determine senescent cells as we previously reported (38, 39).

Western blot analysis

Western blot analyses were performed as previously described (39). Briefly, protein samples were extracted using cell lysis buffer (Cell Signaling) supplemented with a cocktail of proteinase inhibitors (Sigma). The protein concentrations were quantified using a Bio-Rad Dc protein assay kit (Bio-Rad Laboratories, Hercules, CA). Fifty microgram protein samples were resolved on 4 – 20% Mini-Protean TGX gels (Bio-Rad) and transferred onto 0.2 μM PVDF membrane (Millipore). Blots were blocked with 5% non-fat milk for 1–2 hours at room temperature and then probed with primary antibodies and incubated at 4°C overnight. After extensive washing with TBS-T, blots were incubated with appropriate HRP-conjugated secondary antibody for 1.5 h at room temperature. Protein bands were detected using an ECL Plus Western Blotting Detection System (GE Healthcare Life Science).

Immunoprecipitation (IP) and Ubiquitination Assay

SUM159 cells were treated with C1572 (0.2 μM) or DMSO as vehicle control for 2 h. Cell lysates were prepared using RIPA lysis buffer (Santa Cruz). For MYC IP, cell lysates were pre-cleared using 5 μl normal rabbit IgG (sc-2027, Santa Cruz), together with 20 μl protein A/G PLUS-Agarose (Santa Cruz). The pre-cleared lysates were incubated with 5 μl rabbit anti-human c-Myc monoclonal antibodies (Cell Signaling) for 1 h and then with 20 μl protein A/G PLUS-Agarose overnight at 4 degree. Immunoprecipitates were collected by centrifugation and washed with RIPA buffer for 3 times. After final wash, IP products were resuspended in 50 μl SDS loading buffer and resolved on 4 – 20% Mini-Protean TGX gels (Bio-Rad) and transferred onto PVDF membrane (Millipore). Western blots were performed using mouse anti-ubiquitin specific antibodies (Cell Signaling).

Xenograft study

TNBC orthotopic xenografts were established as previously described (8). Briefly, two million SUM159 or MDA-MB-231 cells were mixed with Matrigel (1:1) and transplanted into the 4^{th} mammary fat pad of NOD-SCID-IL_2R gamma^{null} (NSG) mice (Jackson Laboratories). Four weeks after tumor cell implantation when tumor volume reaches ~ 100 mm^3, mice were randomized into three groups and treated with C1572 (0.3 mg/kg or 0.6 mg/kg) or vehicle control, respectively, via intraperitoneal (i.p.) injection three times per week for 3 weeks. Tumor volume was measured weekly using calipers and calculated using the following formula: tumor volume = length × width^2/2. At the end of drug treatment study, animals were euthanized and tumors were surgically removed, weighted and subjected to tissue section preparations and histopathological analyses.

Limited dilution assay (LDA)

Cancer-initiating cells (CICs) in residual tumor cells after drug treatment were assessed using LDA as previously described (37). Briefly, different doses/dilutions (100,000, 10,000, 1, 000 and 100 cells) of SUM159 cells were mixed with Matrigel (1:1) and implanted into

Author Manuscript Author Manuscript Author Manuscript Author Manuscript

the 4th mammary fat pad of NSG mice. The formation of tumors after tumor cell transplantation was examined twice per week for 10 weeks. The frequency of CICs was calculated using L-Calc software (Stem Cell Biotechnologies).

Statistical analysis

Comparisons between groups were carried out using Student's *t*-test. Differences were considered statistically significant at $p < 0.05$. The error bars indicate SEM. All analyses were carried out with the GraphPad Prism program (GraphPad Software, Inc. San Diego, CA).

Results

C1572 depletes TNBC CSCs in a dose-dependent manner

The mammosphere formation assay (MFA) is a useful technique to measure the sphere-forming ability of CSCs and the sphere-initiating cell (SIC) is a surrogate of CSCs in culture (37). To develop novel therapeutic agents that target CSCs, we performed an unbiased screen of 165 small molecule compounds using MFA. Through the screen, we identified 18 compounds that inhibit the formation of mammospheres by 50% or more (Fig. 1A). Among the 18 hits in the screen, C1572 was the top hit, and completely depleted SICs in culture (Fig. 1A–C). To confirm the effect of this compound on CSCs, we investigated the response of sorted $ESA^+/CD44^+/CD24^-$ cells to C1572 treatment. The result showed that at nanomolar concentrations, C1572 significantly inhibited the formation of mammospheres by $ESA^+/CD44^+/CD24^-$ cells, in a dose-dependent manner (Fig. 1D, Supplementary Fig. S1).

To determine if a transient treatment with C1572 is sufficient to inhibit CSCs in TNBC, we incubated human TNBC cells with C1572 overnight (~ 16 h) and then removed the drug and performed MFA to detect CSCs in residual tumor cells. As shown in Fig. 1E & F, even a short period of incubation with C1572 dramatically reduces the number of SICs in both SUM159 and Hs578T residual tumor cells. Similar results were observed in MDA-MB-231 cells (Supplementary Fig. S2A). Notably, C1572 shows no significant effects on human hematopoietic stem and progenitor cells (HSPCs) at doses lethal for CSCs and exhibits only modest inhibitory activity at higher doses (Supplementary Fig. S2B). Taken together, these results suggest that treatment with C1572 selectively depletes TNBC CSCs while sparing normal tissue stem cells such as HSPCs.

C1572 is a potent small molecule inhibitor of MYC

Next, we investigated the mechanisms whereby C1572 depletes TNBC CSCs. Previous studies have shown that MYC, STAT3 and β-catenin are involved in regulating CSC survival and self-renewal functions (40–42). We determined if C1572 treatment impacted the expression of these proteins in TNBC cells. Surprisingly, C1572 dramatically decreased MYC protein levels in SUM159 cells in a dose-dependent manner, but had no significant effects on STAT3, β-catenin and NF-kB p65 expression (Fig. 2A). Similar results were observed in MDA-MB-231 and Hs578T cells (Supplementary Fig. S3A–C). The time course studies indicated that incubation with C1572 led to a reduction in MYC protein levels as early as 2 h, reaching a maximum effect at 4 to 6 h after treatment (Fig. 2B). It is worth

Author Manuscript Author Manuscript Author Manuscript Author Manuscript

noting that MYC protein levels gradually increased and were almost back to normal levels 4 h after drug withdrawal, suggesting that the inhibition effect of C1572 is likely reversible (Supplementary Fig. S3D). However, MYC protein levels decreased again at 24 h after drug removal (Supplementary Fig. S3D). These results suggest that C1572 may induce both acute and long-term MYC inhibition.

To gain insight into the mechanisms by which C1572 inhibits MYC in TNBC cells, we measured MYC mRNA expression levels. The real-time RT-PCR data indicate that C1572 has no significant impact on MYC mRNA levels at doses that deplete MYC protein (Fig. 2C). In contrast, this compound markedly shortened the half-life of MYC protein, suggesting that C1572 may stimulate protein degradation (Fig. 2D; Supplementary Fig. S3E). In agreement with this, we showed that C1572 increased the levels of both phosphorylated and ubiquitinated MYC (Fig. 2E & F). Furthermore, we found that co-treatment with a proteasome inhibitor, MG-132, could rescue the C1572-induced decline in MYC protein (Fig. 2G). These data support the hypothesis that C1572 inhibits MYC via stimulating its post-translational modifications and subsequent degradation.

JQ1 is a well-characterized and commercially available MYC small-molecule inhibitor. It was shown that JQ1 suppresses MYC transcription via interacting with one of the BET proteins, BRD4 (43). Notably, our studies demonstrate that C1572 is 100-fold more potent than JQ1 in inhibiting MYC (Supplementary Fig. S4). More importantly, the observation that C1572 selectively reduces MYC protein levels, but not the expression of several other nuclear proteins including STAT3, β-catenin, p65 and Bmi-1, suggests that this compound has an unusual degree of specificity for MYC (Fig. 2A & B; Supplementary Fig. S3B, C).

To determine if the observed down-regulation of MYC by C1572 was due to cell toxicity or cell cycle arrest, we investigated the impact of several known cytotoxic and chemotherapeutic agents on MYC expression. We found that C1572 was the only compound that completely depleted MYC protein in human TNBC cells, whereas other agents including paclitaxel, etoposide, SN-38, cisplatin, Topotecan, curcumin and AZD8055 did not cause any significant effects on MYC expression (Supplementary Fig. S5). Of note, treatment with C1572 had little effect on tumor cell viability, whereas paclitaxel (Taxol) treatment markedly induced apoptosis (Fig. 2H–J; Supplementary Fig. S6), suggesting that the MYC inhibition activity of C1572 is not due to cell death.

Silencing of MYC expression by siRNA recapitulates the CSC-depletion effect of C1572

To test the hypothesis that C1572 depletes CSCs via targeting MYC, we performed a loss-of-function analysis of the *MYC* oncogene to determine if silencing of MYC expression can phenocopy the effect of C1572 in targeting TNBC CSCs. As shown in Figure 3A, the silencing of MYC by siRNA was confirmed by Western blot analyses. Interestingly, we found that silencing of MYC led to only a modest reduction in the number of viable TNBC cells at 48 h after siRNA transfection (Fig. 3B). In contrast, mammosphere formation assays revealed that knockdown of MYC expression markedly inhibited SICs (a surrogate of CSCs) in SUM159 cells (Fig. 3C & D). Similar results were observed in MDA-MB-231 cells (Fig. 3E). These results demonstrate that silencing of MYC expression phenocopies the CSC-depletion effect of C1572. Together with the data shown in Figures 1 & 2, these new

Author Manuscript Author Manuscript Author Manuscript Author Manuscript

findings strongly support the hypothesis that C1572 eradicates TNBC CSCs via targeting the MYC oncoprotein.

Inhibition of MYC induces senescence in TNBC cells

Although silencing of MYC expression selectively depletes CSCs, it has little effect on the survival of TNBC cells (Fig. 3). These results support the concept that induction of apoptotic cell death is not the primary mechanism underlying MYC knockdown-induced depletion of CSCs. Given the fact that MYC plays a critical role in overriding oncogene RAS-induced senescence (44), we decided to investigate if silencing of MYC induces senescence in human TNBC cells. SA-β-gal assays show that knockdown of MYC expression markedly increases the number of SA-β-gal positive senescent cells (Fig. 4A & B), suggesting that knockdown of MYC induces senescence in TNBC cells. Notably, we found that treatment with C1572 can phenocopy MYC knockdown-induced senescence in SUM159 cells (Fig. 4C & D). Similar results were observed in MDA-MB-231 cells (Fig. 4E). Furthermore, the senescence phenotype was sustained even when C1572 was removed from the culture medium after a short period (14 h) of incubation (Fig. 4F). Taken together, these new findings demonstrate for the first time that knockdown of MYC expression induces senescence in TNBC cells and suggest that targeted inhibition of MYC may represent a novel therapeutic strategy to eradicate CSCs via the induction of stem cell senescence.

Pharmacological inhibition of MYC by C1572 depletes CSCs in TNBC

Having shown that inhibition of MYC by C1572 depletes TNBC CSCs *in vitro* (Fig. 1 & 2), we next sought to confirm the efficacy of C1572 in eradicating CSCs in culture using CSC transplantation analysis, also known as limited dilution assay (LDA). The number of cancer-initiating cells (CICs) in residual TNBC cells after C1572 treatment was determined by LDAs as previously reported (31). After overnight (16 h) treatment with C1572 there were no significant changes in the number of viable SUM159 cells (Fig. 2H–J; Supplementary Fig. S6). However, these viable cells exhibited a significant defect in their ability to form tumors when transplanted into the fat pads of NOD/SCID IL_2R gamma^{null} (NSG) mice (Fig. 5A & B). More importantly, the results of LDAs demonstrate that the frequency of CICs is 0.033 % versus 0.92% in SUM159 cells treated with either C1572 or DMSO, respectively (Fig. 5B & C). These results indicate that the frequency of CICs in cells treated with C1572 is 28-fold lower than that in SUM159 cells treated with DMSO as a vehicle control (Fig. 5C). In addition, we examined the weight of tumors generated from the two groups of cells. The data revealed that C1572-treated TNBC cells produced smaller tumors than cells treated with DMSO (Fig. 5A & D). To assess the number of CSCs in xenograft tumors, we performed mammosphere formation assays using xenograft tumor-derived single cell suspensions. The results showed that the number of SICs was markedly reduced in tumors derived from C1572-treated animals, suggesting that the number of CSCs was significantly lower in xenograft tumors derived from C1572-treated SUM159 cells than in those derived from cells treated with DMSO (Fig. 5E & F). Together, these findings demonstrate for the first time that even a transient inhibition of MYC by C1572 significantly depletes TNBC CSCs, suggesting that targeted inhibition of MYC is likely an effective therapeutic strategy to eradicate therapy-resistant CSCs for TNBC treatment.

Author Manuscript Author Manuscript Author Manuscript Author Manuscript

C1572 suppresses the growth of TNBC xenografts and eliminates CSCs *in vivo*

To evaluate the ability of C1572 to suppress tumor growth and eradicate TNBC CSCs in tumor tissues *in vivo*, we established SUM159 orthotopic xenograft tumors in NSG mice and then treated tumor-bearing mice with a range of doses of C1572 or vehicle (DMSO). Tumor volume analyses indicated that C1572 suppressed the growth of TNBC xenograft tumors in a dose-dependent fashion (Fig. 6A) and the average tumor weight in C1572-treated mice was significantly lower than that of vehicle-treated mice (Fig. 6B & C). To assess the number of CSCs in residual xenograft tumors, xenograft-derived single cells were prepared and mammosphere formation assays were performed to determine the sphere-forming ability of CSCs in residual xenograft tumors after different treatments. We found that the number of SICs was markedly reduced in tumors from C1572-treated mice compared to those treated with vehicle control (Fig. 6D). Similar results were observed using an MDA-MB-231 orthotopic xenograft model (Fig. 6E & F). These findings confirmed the efficacy of C1572 in suppressing tumor growth in vivo and in eliminating CSCs in human TNBC xenografts. Of note, no significant changes in body weight were observed between C1572 treated and vehicle control mice, suggesting that C1572 is well tolerated in NSG mice (Supplementary Fig. 7).

In order to determine the causal correlation between C1572-mediated CSC depletion and MYC inhibition in tumor tissues *in vivo*, IHC analyses were performed to examine MYC expression levels in residual tumors after drug treatment. As shown in Fig. 6G, IHC showed that C1572-mediated CSC depletion correlated with decreased MYC expression in xenograft tumors, suggesting that C1572 suppresses tumor growth and depletes CSCs in tumor tissues via targeting the MYC oncoprotein.

In light of the observation that C1572 suppresses tumor growth in a dose-dependent fashion (Fig. 6A–C), we measured whether an increase in dosing frequency could improve the therapeutic outcome and whether therapy-induced tumor suppression would be sustained post-treatment. As shown in Fig. 6H, increased dosing frequency resulted in complete tumor regression. Equally importantly, C1572-induced tumor regression persists at least three weeks after the final dosing. Together, these results demonstrate for the first time the therapeutic potential of C1572 to induce human TNBC xenograft tumor regression and deplete drug-resistant CSCs in tumor tissues in a preclinical setting.

Discussion

Therapy resistance and tumor recurrence is a major challenge limiting the success of breast cancer treatment, particularly for the TNBC subtype. Growing evidence indicates that CSCs are likely responsible for metastatic progression and tumor relapse via regeneration of new tumors (11). It has been shown that CSCs are selectively enriched in residual tumors following anticancer therapies (7, 8, 13–15), suggesting that the inability of traditional chemotherapy to kill CSCs may contribute to tumor regrowth and treatment failure. Thus, it is critical to develop new therapeutic agents that can effectively target drug-resistant CSCs and improve survival for breast cancer patients. In the present study, using unbiased drug screenings we have identified C1572 as a potential therapeutic agent to target TNBC CSCs. Importantly, we show that treatment with C1572 suppresses TNBC xenograft growth in vivo

Author Manuscript Author Manuscript Author Manuscript Author Manuscript

in a dose-dependent fashion and markedly reduces the number of SICs in residual tumors. Thus, C1572 represents a new lead compound targeting drug-resistant CSCs in TNBC. Furthermore, it appears that there is no significant change in body weight between mice treated with C1572 and those treated with vehicle control, suggesting that this compound is well-tolerated in mice and may have a favorable toxicity profile in possible clinical applications.

The *MYC* oncogene encodes for a transcription factor that is overexpressed in multiple human cancer types, including TNBC (16–21). Functional genomic studies have established a causal role for MYC in tumorigenesis and tumor maintenance, as evidenced by the fact that various tumors are addicted to MYC and that its inactivation leads to tumor regression in multiple preclinical tumor models (45–47). Important to the present study, MYC expression is selectively elevated in basal-like TNBC, elevating the activity of the MYC signaling pathway (20, 21, 48). Earlier efforts to target MYC with small molecules have been difficult, but our present study implies that this approach is a viable strategy to eradicate drug-resistant CSCs in TNBC. The present study provides a proof of principle that pharmacological interference of MYC by C1572 is a new and effective therapeutic approach to target CSCs for TNBC treatment.

It is well documented that senescence induction is an important mechanism of tumor prevention in response to oncogene activation (47, 49). One possible mechanism underlying MYC's pro-tumor properties is likely through antagonizing oncogene activation-induced senescence (44, 47). We, and others, have shown that the induction of premature senescence is a crucial mechanism of action for some therapeutic agents and radiation to induce tumor suppression (38, 39, 50). New data presented here reveal that knockdown of MYC expression has only a modest impact on cell viability, but markedly depletes CSCs in TNBC. Subsequent mechanistic studies indicate that MYC knockdown induces senescence in TNBC cells. These results suggest that inhibition of MYC may deplete CSCs via the induction of senescence in stem cell subpopulation. In agreement with this concept, it has been shown that inactivation of MYC can lead to tumor regression *in vivo* through the induction of senescence in hepatocellular carcinoma and lymphoma cells (47).

Although MYC has been considered an attractive target for cancer treatment (45–47), yet therapeutic agents that target MYC directly have been difficult to develop. Previous studies examining the therapeutic potential of MYC inactivation have been performed largely through genetic approaches (45–47). Recently, attempts have been made to block MYC's function indirectly, such as by inhibiting the key protein-protein interactions (e.g., BET bromodomain inhibition) involved in MYC transcription (43). As a result, JQ1 is available as a commercially available MYC small-molecule inhibitor. Surprisingly, our present study shows C1572 to be 100-fold more potent than JQ1 in inhibiting MYC. Moreover, based upon the fact it has no effects on several other transcription factors, including β-catenin, STAT3, p65 and Bmi-1, we believe that C1572 has fairly robust selectivity.

In summary, we demonstrate for the first time that C1572 selectively depletes drug-resistant CSCs in TNBC via targeting the MYC oncoprotein. Strikingly, C1572 is 100-fold more potent in inhibiting MYC than the commercially available MYC small molecule inhibitor

Author Manuscript Author Manuscript Author Manuscript Author Manuscript

JQ1. Preclinical animal studies revealed that C1572 treatment depletes CSCs in TNBC xenograft tumors and markedly suppresses tumor growth *in vivo*. Furthermore, the CSC-depletion effects of C1572 correlate with a significant reduction of MYC protein levels in residual tumors. These new findings support the development of C1572 as a therapeutic agent to target CSCs for TNBC treatment and also suggest that MYC may be exploited as a biomarker to evaluate the therapeutic response of this compound.

Supplementary Material

Refer to Web version on PubMed Central for supplementary material.

Acknowledgments

Grant Support: This study was supported in part by NIH grants GM103542, HL106451 and UL1TR001450. This work was also partially supported by the Cell & Molecular Imaging Shared Resource of Hollings Cancer Center at the Medical University of South Carolina (P30 CA138313) and the Shared Instrumentation Grant S10 OD018113.

References

1. Siegel R, Naishadham D, Jemal A. Cancer statistics, 2013. CA Cancer J Clin. 2013; 63(1):11–30. [PubMed: 23335087]
2. Sørlie T, Perou CM, Tibshirani R, Aas T, Geisler S, Johnsen H, et al. Gene expression patterns of breast carcinomas distinguish tumor subclasses with clinical implications. Proc Natl Acad Sci U S A. 2001; 98:10869–74. [PubMed: 11553815]
3. Sims AH, Howell A, Howell SJ, Clarke RB. Origins of breast cancer subtypes and therapeutic implications. Nat Clin Pract Oncol. 2007; 4:516–25. [PubMed: 17728710]
4. Bertucci F, Finetti P, Cervera N, Esterni B, Hermitte F, Viens P, Birnbaum D. How basal are triple-negative breast cancers? Int J Cancer. 2008; 123:236–40. [PubMed: 18398844]
5. Liedtke C, Mazouni C, Hess KR, André F, Tordai A, Mejia JA, et al. Response to neoadjuvant therapy and long-term survival in patients with triple-negative breast cancer. J Clin Oncol. 2008; 26:1275–81. [PubMed: 18250347]
6. Rivera E. Management of metastatic breast cancer: monotherapy options for patients resistant to anthracyclines and taxanes. Am J Clin Oncol. 2010; 33:176–85. [PubMed: 19675449]
7. Creighton CJ, Li X, Landis M, Dixon JM, Neumeister VM, et al. Residual breast cancers after conventional therapy display mesenchymal as well as tumor-initiating features. Proc Natl Acad Sci U S A. 2009; 106:13820–5. [PubMed: 19666588]
8. Bhola NE, Balko JM, Dugger TC, Kuba MG, Sánchez V, Sanders M, et al. TGF-β inhibition enhances chemotherapy action against triple-negative breast cancer. J Clin Invest. 2013; 123:1348–58. [PubMed: 23391723]
9. Singh SK, Hawkins C, Clarke ID, Squire JA, Bayani J, Hide T, et al. Identification of human brain tumor initiating cells. Nature. 2004; 432:396–401. [PubMed: 15549107]
10. Al-Hajj M, Wicha MS, Benito-Hernandez A, Morrison SJ, Clarke MF. Prospective identification of tumorigenic breast cancer cells. Proc Natl Acad Sci U S A. 2003; 100:3983–8. [PubMed: 12629218]
11. Adorno-Cruz V, Kibria G, Liu X, Doherty M, Junk DJ, Guan D, et al. Cancer stem cells: targeting the roots of cancer, seeds of metastasis, and sources of therapy resistance. Cancer Res. 2015; 75:924–9. [PubMed: 25604264]
12. Liu H, Patel MR, Prescher JA, Patsialou A, Qian D, Lin J, et al. Cancer stem cells from human breast tumors are involved in spontaneous metastases in orthotopic mouse models. Proc Natl Acad Sci U S A. 2010; 107:18115–20. [PubMed: 20921380]
13. Kurtova AV, Xiao J, Mo Q, Pazhanisamy S, Krasnow R, Lerner SP, et al. Blocking PGE2-induced tumour repopulation abrogates bladder cancer chemoresistance. Nature. 2015; 517:209–13. [PubMed: 25470039]

Author Manuscript Author Manuscript Author Manuscript Author Manuscript

14. Calcagno AM, Salcido CD, Gillet JP, Wu CP, Fostel JM, Mumau MD, et al. Prolonged drug selection of breast cancer cells and enrichment of cancer stem cell characteristics. J Natl Cancer Inst. 2010; 102:1637–52. [PubMed: 20935265]
15. Liu YP, Yang CJ, Huang MS, Yeh CT, Wu AT, Lee YC, et al. Cisplatin selects for multidrug-resistant CD133+ cells in lung adenocarcinoma by activating Notch signaling. Cancer Res. 2013; 73:406–16. [PubMed: 23135908]
16. Felsher DW, Bishop JM. Reversible tumorigenesis by MYC in hematopoietic lineages. Mol Cell. 1999; 4:199–207. [PubMed: 10488335]
17. Adhikary S, Eilers M. Transcriptional regulation and transformation by Myc proteins. Nat Rev Mol Cell Biol. 2005; 6:635–45. [PubMed: 16064138]
18. Alles MC, Gardiner-Garden M, Nott DJ, Wang Y, Foekens JA, Sutherland RL, et al. Meta-analysis and gene set enrichment relative to er status reveal elevated activity of MYC and E2F in the "basal" breast cancer subgroup. PLoS One. 2009; 4:e4710. [PubMed: 19270750]
19. Xu J, Chen Y, Olopade OI. MYC and Breast Cancer. Genes Cancer. 2010; 1:629–40. [PubMed: 21779462]
20. Horiuchi D, Kusdra L, Huskey NE, Chandriani S, Lenburg ME, Gonzalez-Angulo AM, et al. MYC pathway activation in triple-negative breast cancer is synthetic lethal with CDK inhibition. J Exp Med. 2012; 209:679–696. [PubMed: 22430491]
21. Chandriani S, Frengen E, Cowling VH, Pendergrass SA, Perou CM, Whitfield ML, Cole MD. A core MYC gene expression signature is prominent in basal-like breast cancer but only partially overlaps the core serum response. PLoS One. 2009; 4:e6693. [PubMed: 19690609]
22. He TC, Sparks AB, Rago C, Hermeking H, Zawel L, da Costa LT, et al. Identification of c-MYC as a target of the APC pathway. Science. 1998; 28:1509–12.
23. DiMeo TA, Anderson K, Phadke P, Fan C, Perou CM, Naber S, Kuperwasser C. A novel lung metastasis signature links Wnt signaling with cancer cell self-renewal and epithelial-mesenchymal transition in basal-like breast cancer. Cancer Res. 2009; 69:5364–5373. [PubMed: 19549913]
24. Takahashi K, Yamanaka S. Induction of pluripotent stem cells from mouse embryonic and adult fibroblast cultures by defined factors. Cell. 2006; 126:663–76. [PubMed: 16904174]
25. Moumen M, Chiche A, Decraene C, Petit V, Gandarillas A, Deugnier MA, et al. Myc is required for β-catenin-mediated mammary stem cell amplification and tumorigenesis. Mol Cancer. 2013; 12:132. [PubMed: 24171719]
26. Leuenroth SJ, Okuhara D, Shotwell JD, Markowitz GS, Yu Z, Somlo S, Crews CM. Triptolide is a traditional Chinese medicine-derived inhibitor of polycystic kidney disease. Proc Natl Acad Sci U S A. 2007; 104:4389–94. [PubMed: 17360534]
27. Tao XL, Sun Y, Dong Y, et al. A prospective, controlled, double-blind, cross-over study of Tripterygium wilfodii hook F in treatment of rheumatoid arthritis. Chin Med J (Engl). 1989; 102:327–332. [PubMed: 2509153]
28. Qin WZ, Zhu GD, Yang SM, Han KY, Wang J. Clinical observations on Tripterygium wilfordii in treatment of 26 cases of discoid lupus erythematosus. J Tradit Chin Med. 1983; 3:131–132. [PubMed: 6555446]
29. Jiang X. Clinical observations on the use of the Chinese herb Tripterygium wilfordii Hook for the treatment of nephrotic syndrome. Pediatr Nephrol. 1994; 8:343–344. [PubMed: 7917863]
30. Chugh R, Sangwan V, Patil SP, Dudeja V, Dawra RK, Banerjee S, et al. A preclinical evaluation of Minnelide as a therapeutic agent against pancreatic cancer. Sci Transl Med. 2012; 4:156ra139.
31. Kim HJ, Ravichandran K, Ozkok A, et al. The Water-Soluble Triptolide Derivative PG490-88 Protects against Cisplatin-Induced Acute Kidney Injury. J Pharmacol Exp Ther. 2014; 349:518–525. [PubMed: 24727856]
32. Shao Q, Kannan A, Lin Z, Stack BC Jr, Suen JY, Gao L. BET protein inhibitor JQ1 attenuates Myc-amplified MCC tumor growth in vivo. Cancer Res. 2014; 74:7090–102. [PubMed: 25277525]
33. Streicher KL, Willmarth NE, Garcia J, Boerner JL, Dewey TG, Ethier SP. Activation of a nuclear factor kappaB/interleukin-1 positive feedback loop by amphiregulin in human breast cancer cells. Mol Cancer Res. 2007; 5:847–61. [PubMed: 17670913]

Author Manuscript Author Manuscript Author Manuscript Author Manuscript

34. Neve RM, Chin K, Fridlyand J, Yeh J, Baehner FL, Fevr T, et al. A collection of breast cancer cell lines for the study of functionally distinct cancer subtypes. Cancer Cell. 2006; 10:515–27. [PubMed: 17157791]
35. Dontu G, Abdallah WM, Foley JM, Jackson KW, Clarke MF, Kawamura MJ, Wicha MS. In vitro propagation and transcriptional profiling of human mammary stem/progenitor cells. Genes Dev. 2003; 17:1253–70. [PubMed: 12756227]
36. Ponti D, Costa A, Zaffaroni N, Pratesi G, Petrangolini G, Coradini D, et al. Isolation and in vitro propagation of tumorigenic breast cancer cells with stem/progenitor cell properties. Cancer Res. 2005; 65:5506–11. [PubMed: 15994920]
37. Kreso A, van Galen P, Pedley NM, Lima-Fernandes E, Frelin C, Davis T, et al. Self-renewal as a therapeutic target in human colorectal cancer. Nat Med. 2014; 20:29–36. [PubMed: 24292392]
38. Luo H, Yang A, Schulte BA, Wargovich MJ, Wang GY. Resveratrol Induces Premature Senescence in Lung Cancer Cells via ROS-Mediated DNA Damage. PLoS One. 2013; 8:e60065. [PubMed: 23533664]
39. Luo H, Yount C, Lang H, Yang A, Riemer EC, Lyons K, et al. Activation of p53 with Nutlin-3a radiosensitizes lung cancer cells via enhancing radiation-induced premature senescence. Lung Cancer. 2013; 81:167–73. [PubMed: 23683497]
40. Civenni G, Malek A, Albino D, Garcia-Escudero R, Napoli S, Di Marco S, et al. RNAi-mediated silencing of Myc transcription inhibits stem-like cell maintenance and tumorigenicity in prostate cancer. Cancer Res. 2013; 73:6816–27. [PubMed: 24063893]
41. Marotta LL, Almendro V, Marusyk A, Shipitsin M, Schemme J, Walker SR, et al. The JAK2/STAT3 signaling pathway is required for growth of $CD44^{+}CD24^{-}$ stem cell-like breast cancer cells in human tumors. J Clin Invest. 2011; 121:2723–35. [PubMed: 21633165]
42. Jang GB, Hong IS, Kim RJ, Lee SY, Park SJ, Lee ES, et al. Wnt/β-catenin small molecule inhibitor CWP232228 preferentially inhibits the growth of breast cancer stem-like cells. Cancer Res. 2015; 75:1691–702. [PubMed: 25660951]
43. Delmore JE, Issa GC, Lemieux ME, Rahl PB, Shi J, Jacobs HM, et al. BET bromodomain inhibition as a therapeutic strategy to target c-Myc. Cell. 2011; 146:904–17. [PubMed: 21889194]
44. Hydbring P, Bahram F, Su Y, Tronnersjö S, Högstrand K, von der Lehr N, et al. Phosphorylation by Cdk2 is required for Myc to repress Ras-induced senescence in cotransformation. Proc Natl Acad Sci U S A. 2010; 107:58–63. [PubMed: 19966300]
45. Jain M, Arvanitis C, Chu K, Dewey W, Leonhardt E, Trinh M, et al. Sustained loss of a neoplastic phenotype by brief inactivation of MYC. Science. 2002; 297:102–4. [PubMed: 12098700]
46. Soucek L, Whitfield J, Martins CP, Finch AJ, Murphy DJ, Sodir NM, et al. Modelling Myc inhibition as a cancer therapy. Nature. 2008; 455:679–83. [PubMed: 18716624]
47. Wu CH, van Riggelen J, Yetil A, Fan AC, Bachireddy P, Felsher DW. Cellular senescence is an important mechanism of tumor regression upon c-Myc inactivation. Proc Natl Acad Sci U S A. 2007; 104:13028–33. [PubMed: 17664422]
48. Camarda R, Zhou AY, Kohnz RA, Balakrishnan S, Mahieu C, Anderton B, et al. Inhibition of fatty acid oxidation as a therapy for MYC-overexpressing triple-negative breast cancer. Nat Med. 2016; 22:427–32. [PubMed: 26950360]
49. Braig M, Lee S, Loddenkemper C, Rudolph C, Peters AH, Schlegelberger B, et al. Oncogene-induced senescence as an initial barrier in lymphoma development. Nature. 2005; 436:660–5. [PubMed: 16079837]
50. Acosta JC, Gil J. Senescence: a new weapon for cancer therapy. Trends Cell Biol. 2012; 22(4): 211–9. [PubMed: 22245068]

Author Manuscript Author Manuscript Author Manuscript Author Manuscript

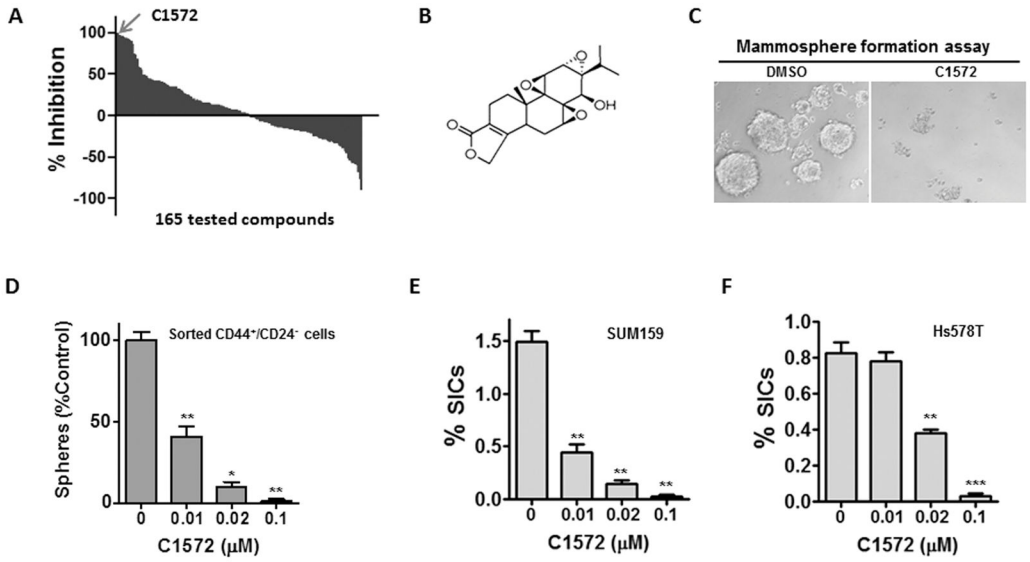

Fig. 1. C1572 depletes TNBC CSCs in a dose-dependent manner

A, Mammosphere formation assay (MFA) was employed to screen new agents that target CSCs. Shown is the waterfall plot of the screening results, the arrow indicating the position of C1572 on the plot. **B,** The chemical structure of C1572. **C,** Representative images of MFA depicting that C1572 depletes SICs in culture. **D,** Sorted $ESA^{+}/CD44^{high}/CD24^{low}$ cells were used for MFA to validate the ability of C1572 to target CSCs. **E & F,** The frequency of SICs in residual SUM159 and Hs578T cells following different doses of C1572 treatment is presented as mean ± SEM of three independent experiments. * $p< 0.05$, ** $p< 0.01$, *** $p< 0.001$ vs. vehicle (DMSO) control.

Author Manuscript
Author Manuscript
Author Manuscript
Author Manuscript

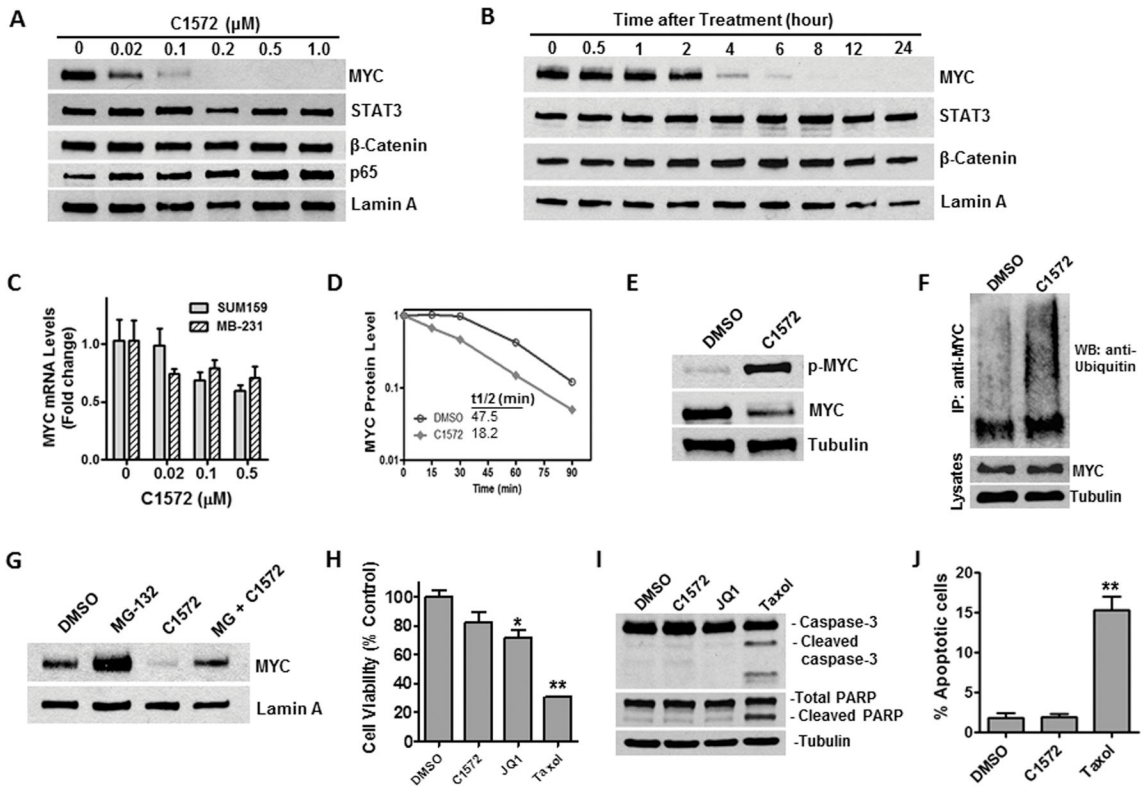

Fig. 2. C1572 selectively inhibits MYC in TNBC cells

A, Expression levels of MYC, STAT3, β-catenin and p65 in SUM159 cells were determined by Western blot analyses at 16 h after C1572 treatments. **B,** Expression levels of MYC, STAT3 and β-catenin at different times after C1572 (0.2 μM) treatment were analyzed by Western blot. **C,** MYC mRNA levels in SUM159 and MB-231 cells were determined using real-time RT-PCR at 6 h after C1572 treatment. **D,** SUM159 cells were treated with C1572 (0.2 μM) for 2 h and then cycloheximide (CHX, 50 μg/ml) was added to stop translation. MYC protein levels at different time points after CHX treatment were quantified and plotted. **E,** Phosphorylated MYC (Ser62) was determined by immunoblotting. **F,** SUM159 cells were treated with C1572 (0.2 μM) for 2 h and MYC protein pulled down by immunoprecipitation (IP). Ubiquitinated MYC was determined by Western blot using ubiquitin specific monoclonal antibodies. **G,** Treatment with a proteasome inhibitor MG-132 (5 μM) attenuates C1572-induced MYC degradation. MYC levels were determined by Western blots at 6 h after C1572 and/or MG-132 treatment. **H**, SUM159 cells were treated with C1572 (0.2 μM), JQ1 (10 μM), Taxol (0.1 μM) or DMSO as vehicle control. Cell viability was determined using MTS assays 24 h after drug treatment. **I,** SUM159 cells were treated as described in H. Cleaved caspase-3 and PARP were determined using Western blot. **J,** Apoptosis was measured using an Annexin V Apoptosis Detection Kit (BD Biosciences) and flow cytometry 24 h after drug treatments. * $p < 0.05$; ** $p < 0.01$ vs. DMSO control.

Author Manuscript
Author Manuscript
Author Manuscript
Author Manuscript

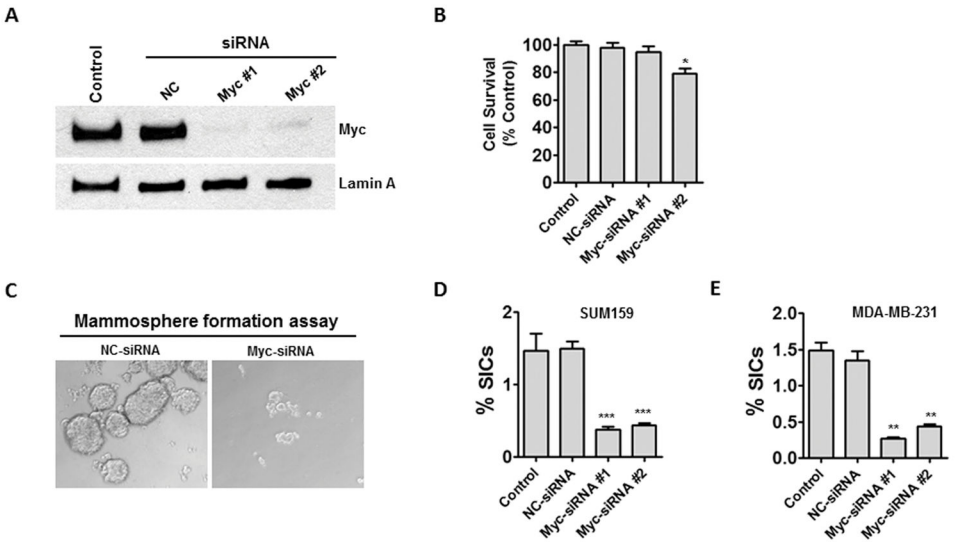

Fig. 3. MYC is required for TNBC CSC survival

A, SUM159 cells were transfected with MYC siRNA (10 nM) or non-targeting control (NC)-siRNA using Lipofectamine RNAi MAX (Invitrogen) according to the manufacturer's instructions. The knockdown of MYC by siRNA was examined by Western blot analyses at 48 h after transfection. **B,** The number of viable SUM159 cells was determined and normalized to the percentage of mock transfection control cells at 48 h after transfection. **C,** Tumor sphere formation assays were performed to determine the frequency of SICs. **D,** The frequency of SICs in SUM159 cells with or without MYC knockdown was determined and is presented as mean ± SEM. **E,** The frequency of SICs in MDA-MB-231 cells following MYC knockdown was determined and is presented as mean ± SEM. * $p < 0.05$ vs. NC-siRNA; ** $p < 0.01$ vs. NC-siRNA; *** $p < 0.001$ vs. NC-siRNA.

Author Manuscript Author Manuscript Author Manuscript Author Manuscript

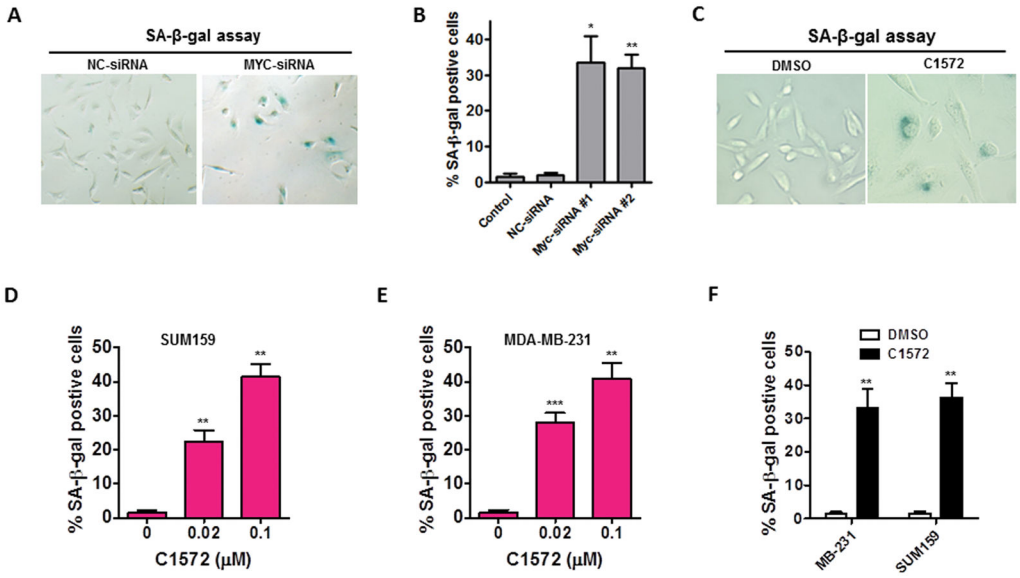

Fig. 4. Silencing of MYC induces senescence in TNBC cells

A, SUM159 cells were transfected with MYC siRNA (10 nM) or non-targeting control (NC)-siRNA using Lipofectamine RNAi MAX (Invitrogen) as shown in Figure 3. Senescent cells were identified 6 days after siRNA transfection by SA-β-gal staining as previously reported (38, 39). **B**, The percentage of SA-β-gal positive senescent cells is presented as mean ± SEM of three independent experiments. **C,** Shown are representative images of senescent cells following C1572 treatment. **D & E,** Senescent SUM159 and MB-231 cells were determined by SA-β-gal assays at 6 days after C1572 treatment. **F,** SUM159 cells and MB-231 cells were treated with C1572 (0.1 μM) and the drug was removed after 14 h of incubation. Senescent cells were determined by SA-β-gal staining at 5 days after drug treatment. * $p < 0.05$; ** $p < 0.01$; *** $p < 0.001$ vs. NC-siRNA or vehicle (DMSO) control.

Author Manuscript Author Manuscript Author Manuscript Author Manuscript

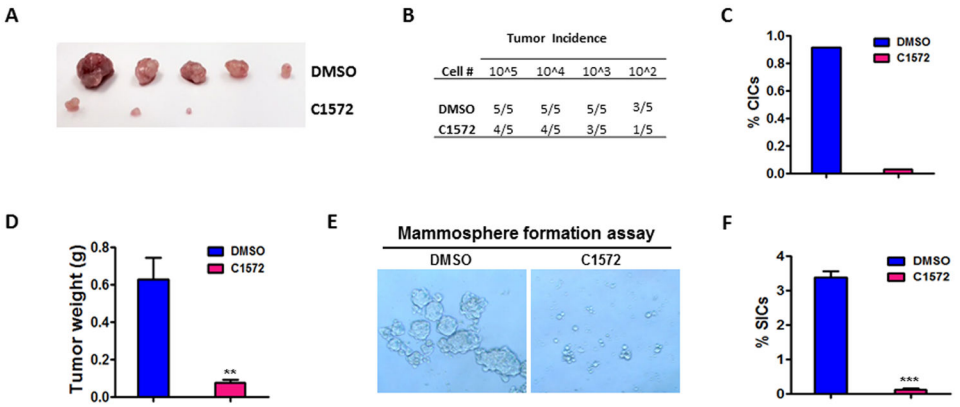

Fig. 5. C1572 treatment depletes CSCs in TNBC

A, SUM159 cells were treated with C1572 (0.1 μM) or DMSO as control for 16 h. LDAs were performed to examine CICs in residual tumor cells that survived the treatment. Shown are representative photographs of xenograft tumors derived from DMSO-treated (upper panel) and C1572-treated (lower panel) SUM159 cells, respectively. **B,** Tumor incidence in mice transplanted with SUM159 cells after C1572 or DMSO treatments was monitored for 10 weeks. **C,** The frequency of CICs from LDAs was calculated using L-Calc software (StemCell Biotechnologies, Inc.). **D,** Average tumor weights are presented as mean +/− SEM (n=5). **E,** Xenograft-derived single cells were prepared by enzymatic dissociation using collagenase/hyaluronidase (StemCell Technologies, Inc.) according to the manufacturer's protocol. Shown are representative photographs of tumor sphere assays of single suspension cells derived from SUM159 xenograft tumors. **F,** The frequency of SICs in xenograft tumors is presented as mean +/− SEM. ** $p < 0.01$, *** $p < 0.001$ vs. DMSO control.

Author Manuscript Author Manuscript Author Manuscript Author Manuscript

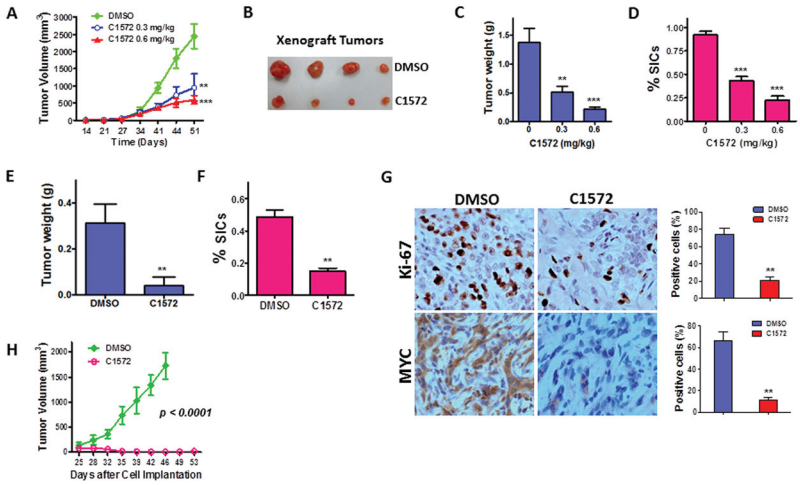

Fig. 6. C1572 suppresses tumor growth and eliminates CSCs in TNBC xenografts

A, C1572 suppresses SUM159 orthotopic xenograft tumor growth in a dose-dependent fashion. Tumor bearing mice (n= 6) were treated with C1572 at the indicated doses via i.p. injection three times per week for 3 weeks. **B,** Representative images of SUM159 orthotopic xenografts are presented. **C,** C1572 treatment reduces tumor weight of SUM159 xenografts. **D,** The number of SICs was significantly decreased in residual tumors after C1275 treatment. **E,** C1572 treatment reduces tumor weight of MDA-MB-231 xenografts. **F,** The number of SICs was decreased significantly in residual tumors of MDA-MB-231 xenografts after C1275 treatment. **G,** MYC and Ki-67 expression levels were determined in residual tumor tissues by IHC analyses. **H,** Mice bearing SUM159 orthotopic xenograft tumors (n = 6) were treated with C1572 (0.6 mg/kg, daily i.p. injection) for 2 weeks. Measuring tumor growth was continued for 3 weeks after the final dosing. ** $p< 0.01$, *** $p< 0.001$ vs. DMSO control.